Strongly correlated 2D quantum phases with cold polar molecules: controlling the shape of the interaction potential

H. P. Büchler[1,2], E. Demler[3], M. Lukin[3], A. Micheli[1,2], N. Prokof'ev[4], G. Pupillo[1,2], and P. Zoller[1,2]

[1]*Institute for Theoretical Physics, University of Innsbruck, 6020 Innsbruck, Austria*
[2]*Institute for Quantum Optics and Quantum Information, 6020 Innsbruck, Austria*
[3]*Harvard University, Department of Physics, Cambridge, USA and*
[4]*BEC-INFM, Dipartimento di Fisica, Universit di Trento, I-38050 Povo, Italy*
(Dated: February 6, 2008)

We discuss techniques to tune and shape the long-range part of the interaction potentials in quantum gases of polar molecules by dressing rotational excitations with static and microwave fields. This provides a novel tool towards engineering strongly correlated quantum phases in combination with low dimensional trapping geometries. As an illustration, we discuss a 2D crystalline phase, and a superfluid-crystal quantum phase transition.

The outstanding feature of cold atomic and molecular quantum gases is the high control and tunability of microscopic system parameters via external fields. Prominent examples are the realization of low-dimensional trapping geometries, and the tuning of the contact interaction via Feshbach resonances [1]. In this letter we extend this control to the *shape* and the *strength* of interactions with the goal to generate new classes of potentials. In combination with low-dimensional trapping, these provide a framework for realizing new many body quantum phases and phase transitions. We elaborate these ideas in the context of polar molecules prepared in their electronic and vibrational ground states [2].

Cold polar molecules have attracted significant theoretical interest, in particular in the context of dilute bosonic dipolar quantum gases [3, 4]. Special focus was on the appearance of thermodynamic instabilities and roton softening for weakly interacting gases [5]. Below we are specifically interested in polar molecules in *the strong interaction limit*, where the stability of the dipolar gas is guaranteed by a confinement of the particles into a two-dimensional (2D) setup. We show, that applying appropriately chosen static and/or microwave fields allow us to design effective potentials $V_{\text{eff}}^{\text{2D}}(\mathbf{R})$ between pairs of molecules (see Fig. 1(a)). In turn, these potentials give rise to interesting new many-body phenomena. As an illustration, we consider the appearance of a crystalline phase, and an associated quantum melting to a superfluid phase, for a 2D dipolar interaction $V_{\text{eff}}^{\text{2D}}(\mathbf{R}) = D/R^3$. The interaction strength is characterized by the ratio between the interaction energy and the kinetic energy $r_d = Dm/\hbar^2 a$ with a the average interparticle distance. We determine the transition point $r_{\text{QM}} = 18 \pm 4$ of this superfluid to solid quantum phase transition via Path Integral Monte Carlo simulations. We find that realistic experimental parameters of polar molecules allow for the realization of this quantum phase, which has never been observed so far with cold atomic or molecular gases.

We consider heteronuclear molecules prepared in their electronic and vibrational ground states. We focus on bosonic molecules with a closed electronic shell $^1\Sigma(\nu =$
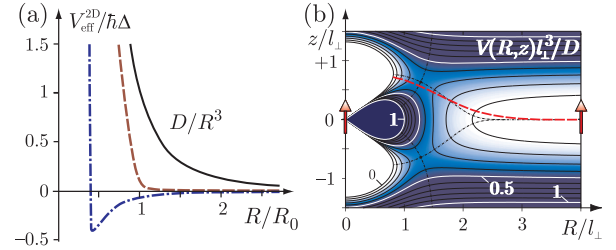

FIG. 1: (a) Effective potentials: dipole potential induced by a static electric field $V_{\text{eff}}^{\text{2D}} = D/R^3$ (solid line); potential with a single microwave transition with $\Omega/\Delta = 0.1$ (dashed line); attractive potential induced by an additional microwave coupling to the states $|1, \pm 1\rangle$ with $\Delta_\perp = 100\Delta$ and $\Omega_\perp/\Delta_\perp = 0.3$ (dash-dotted line). (b) Contour plot of the potential $V(\mathbf{r}) \, l_\perp^3/D$ (Eq. 1) in the (R, z)-plane. The instanton solution is shown as dashed line.

$0)$, e.g. of the type SrO, RbCs or LiCs, as most relevant in present experiments [2]. The Hamiltonian for a single molecule i is $H^{(i)} = \mathbf{p}_i^2/2m + V_{\text{trap}}(\mathbf{r}_i) + H_{\text{rot}}^{(i)} - \mathbf{d}_i\mathbf{E}(t)$. The first two terms are the kinetic energy and the trapping potential for the center-of-mass motion of the molecule of mass m. The term $H_{\text{rot}}^{(i)}$ describes the internal low energy excitations of the molecule, i.e., the rotational degree of freedom of the molecular axis. This term is well described by a rigid rotor $H_{\text{rot}}^{(i)} = B\mathbf{J}_i^2$ with B the rotational constant (in the few to tens of GHz regime) and $\mathbf{J}_i$ the dimensionless angular momentum. The rotational states $|J, M\rangle$ with quantization axis z, and with eigenenergies $BJ(J+1)$ are coupled by a static or microwave field $\mathbf{E}$ via the electric dipole moment $\mathbf{d}_i$ (typically of the order of a few Debye). We assume a setup where the molecules are confined to a 2D configuration in the x, y-plane by a tight harmonic trapping potential $m\omega_\perp^2 z_i^2/2$ with $\omega_\perp = \hbar/ma_\perp^2$, as provided by an optical potential. We remark that the different dynamic polarizabilities parallel and perpendicular to the molecular axis give rise to tensorshifts, which provide an additional (small) state dependent potential for excited rotational states [6].

The interaction of two polar molecules at distance $r = |\mathbf{r}| = |\mathbf{r}_1 - \mathbf{r}_2|$ is described by the Hamiltonian $H = \sum_{i=1}^{2} H^{(i)} + V_{dd}$ with the dipole-dipole interaction $V_{dd} = [\mathbf{d}_1\mathbf{d}_2 - 3(\mathbf{d}_1\mathbf{n})(\mathbf{d}_2\mathbf{n})]/r^3$ and $\mathbf{n} = \mathbf{r}/r$ as unit vector [3]. In the absence of external fields $\mathbf{E}$, the interaction of two molecules in their rotational ground state is determined by the van der Waals attraction $V_{vdW} \sim -C_6/r^6$ with $C_6 \approx d^4/6B$, valid outside of the molecular core region $r > r_{rot} \equiv (d^2/B)^{1/3}$. By dressing with an external field $\mathbf{E}$, we induce and design long-range interactions. On a formal level the derivation of the effective interaction proceeds in two steps: (i) We derive a set of Born-Oppenheimer (BO) potentials by first separating into center-of-mass and relative coordinates, and diagonalizing the Hamiltonian for the relative motion for fixed molecular positions $\mathbf{r}$, $H_{rel} \equiv \sum_{i=1,2}(H_{rot}^{(i)} - \mathbf{d}_i\mathbf{E}) + V_{dd}$. Within an adiabatic approximation, the corresponding eigenvalues play the role of an effective $V_{eff}^{3D}(\mathbf{r})$ interaction potential in a given state manifold dressed by the external field [11]. (ii) We eliminate the motional degrees of freedom in the tightly confined z direction to obtain an effective 2D dynamics with interaction $V_{eff}^{2D}(\mathbf{R})$. In the following we consider the cases of a static field and a microwave field coupling the lowest rotor states.

A *static electric field* applied perpendicular to the trap plane, $\mathbf{E} = E_z\mathbf{e}_z$, polarizes the rotational ground state of each molecule, and induces finite dipole moments $\langle\mathbf{d}_i\rangle \equiv \sqrt{D}\mathbf{e}_z$. These give rise to a long-range dipole-dipole interaction, $V_{eff}^{3D}(\mathbf{r}) = D(r^2 - 3z^2)/r^5$, where D is tunable by the field strength E_z. This expression of interacting dipoles aligned by the external field is valid for distances larger than $r > r_\star$ with $r_\star$ defined by $C_6/r_\star^6 \sim D/r_\star^3$. Furthermore, for $r > r_{rot}$ the BO approximation is easily fulfilled. The combination of the dipole-dipole interaction and the transverse trapping potential implies an interparticle potential

$$V(\mathbf{r}) = \frac{D}{l_\perp^3}\left[\frac{l_\perp^3}{r^3} - 3\frac{z^2 l_\perp^3}{r^5} + \frac{z^2}{2l_\perp^2}\right] \quad (1)$$

with $l_\perp = (Dm/2\hbar^2 a_\perp)^{1/5}a_\perp$ (see Fig. 1(b)), and where we require $l_\perp \gg \max(r_\star, r_{rot})$. The above potential has a saddle point at $R_s \approx 1.28 l_\perp$ and $z_s \approx \pm 0.64 l_\perp$ with the potential height $V_s \approx 0.34D/l_\perp^3$. As a consequence, the short distance regime, $r < l_\perp$, is separated by a potential barrier from the large distance regime, $r > l_\perp$. Within a semi-classical approximation, the tunneling rate through this barrier takes the form $\Gamma = \omega_p \exp[-c(Dm/2\hbar^2 a_\perp)^{2/5}]$ with $c \approx 5.86$ and $\omega_p \sim \sqrt{D/ma^5}$ the "attempt frequency". Therefore, in the strongly interacting limit with a tight confinement the tunneling rate is exponentially suppressed, and the probability to find two particles at a distance $r < l_\perp$ is negligible, and guarantees the stability of an ensemble of polar molecules. Then, the system is completely determined by the interaction potential at large distances

$r \gg l_\perp$, which is in particular also much larger than the short distances scales $r_\star, r_{rot}$. Thus we can reduce the interaction to an effective 2D potential by integrating out the fast transverse motion as

$$V_{eff}^{2D}(\mathbf{R}) = \int dz_1 \int dz_2 |\psi_\perp(z_1)|^2 |\psi_\perp(z_2)|^2 V_{eff}^{3D}(\mathbf{r}), \quad (2)$$

where $\psi_\perp(z_i) = \exp(-z_i^2/2a_\perp^2)/(\pi a_\perp^2)^{1/4}$ is the ground state harmonic oscillator wave-function in the tightly confined z-direction, and is valid for distance $R > (D/\hbar\omega_\perp)^{1/3}$ (note, that $l_\perp \sim (D/\hbar\omega_\perp)^{1/3}$ for realistic parameters). Therefore, the effective 2D interaction reduces to $V_{eff}^{2D} \sim D/R^3$ for large separations $R \gg l_\perp$.

Microwave fields can drive the transition of a molecule from the ground to the first excited rotational state. We denote the corresponding Rabi frequency by Ω and the detuning by Δ. In the weak driving limit $\Omega < \Delta$ the molecules are essentially in their rotational ground state with AC Stark shifted energy and a small admixture from the excited state. For two molecules approaching each other and blue detuning $\Delta > 0$ (cf. Fig. 2), the microwave field will be resonant at distance R_0 with $d^2/R_0^3 \sim \hbar\Delta$, i.e., the ground and first excited rotational states will be strongly mixed. This gives rise to an effective BO potential, which for $r < R_0$ exhibits a strong repulsion inherited from the $\sim 1/r^3$ excited state dipole-dipole interactions; Similar ideas have been discussed as "blue shield" in the context of alkali atoms [7].
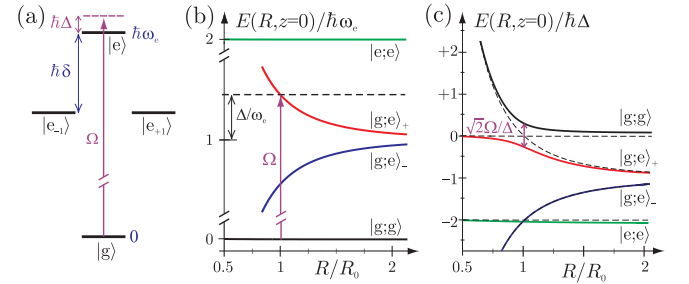

FIG. 2: (a) Energy levels of the rotor in a weak electric field. The microwave transition with detuning Δ and Rabi frequency Ω is shown as the arrow. (b) BO potentials for the internal states for $\Omega = 0$, where $|g;e\rangle_\pm \equiv (|g;e\rangle \pm |e;g\rangle)/\sqrt{2}$ denote the gerade/ungerade first excited states. (c) Avoided level crossing due to the microwave coupling with the effective BO potential V_{eff}^{3D} given by the highest eigenenergy state.

As an example, we consider a microwave field with polarization along the z-axis, driving the transition between the ground state and the first excited state with $M = 0$. Excitations into higher states are suppressed due to the anharmonicity of the spectrum, and spontaneous emission is irrelevant in the microwave regime. The interaction Hamiltonian also couples the excited state $|1,0\rangle$ to the states $|1,\pm1\rangle$ for non-vanishing z (note that such a coupling can also be induced by the tensor shift). In

the following, we suppress this coupling by introducing a (weak) static electric field $E_z \ll B/d$ lifting the degeneracy of the $J = 1$ manifold by $\delta \gg \Delta$, see Fig. 2(a-b), and we focus on distances $r > r_\delta = (d^2/\hbar\delta)^{1/3}$. For each polar molecule, the system reduces to a two level system with the ground state $|g\rangle$ and the first excited state $|e\rangle$ ($M = 0$) dressed by the electric field, and energy difference $\hbar\omega_e$. In a rotating frame the Hamiltonian $H_{\rm rel}$ expressed in the basis $\{|g;g\rangle, |g;e\rangle, |e;g\rangle, |e;e\rangle\}$ becomes

$$H_{\rm rel} = \hbar \begin{bmatrix} D_g\nu(\mathbf{r}) & \Omega & \Omega & 0 \\ \Omega & -\Delta & D\nu(\mathbf{r}) & \Omega \\ \Omega & D\nu(\mathbf{r}) & -\Delta & \Omega \\ 0 & \Omega & \Omega & D_e\nu(\mathbf{r}) - 2\Delta \end{bmatrix}, \quad (3)$$

where $D_g = |\langle g|\mathbf{d}_i|g\rangle|^2$ and $D_e = |\langle e|\mathbf{d}_i|e\rangle|^2$ denote the weak dipole interaction induced by the static field E_z, while $D \approx d^2/3$ accounts for the dipole transition element between the ground and excited state, and $\nu(\mathbf{r}) = (r^2 - 3z^2)/\hbar r^5$ is the shape of the dipole interaction. The effective BO potential $V_{\rm eff}^{\rm 3D}(\mathbf{r})$ derives now from the eigenenergy of the state adiabatically connecting to $|g,g\rangle$ for $r \to \infty$, and is given by the highest energy level, see Fig. 2(c). We find that for a detuning Δ with $R_0 = (D/\hbar\Delta)^{1/3} \gg l_\perp \gtrsim r_\delta$ the combination of the transverse trapping potential with $V_{\rm eff}^{\rm 3D}$ provides again a large tunneling barrier separating the short distance regime from the long distance regime. We emphasize that the existence of this barrier makes the system stable – in contrast to the incomplete shielding discussed previously in the context of "blue shielding" with lasers [7]. Then, in analogy to the discussion of the static electric field, we obtain the effective 2D potential via integrating out the transverse motion; the effective potential $V_{\rm eff}^{\rm 2D}$ is shown in Fig. 1(a). The distance R_0 separates a weakly interacting regime at large distances $R > R_0$ with $V_{\rm eff}^{\rm 2D} \sim \left[(2\Omega^2/\Delta^2)D + D_g\right]/R^3$ from a strongly repulsive regime with $V_{\rm eff}^{\rm 2D} \sim D/R^3$ on distances $l_\perp < R < R_0$.

The BO approximation above is valid as long as the passage through the level crossing at R_0 is adiabatic. For a realistic setup with average interparticle distance $a \sim R_0$, the average particle velocity can be estimated as $\hbar/R_0 m$. Then, the Landau-Zener probability for a diabatic crossing reduces to $P_{\rm LZ} = \exp\left[-2\pi(Dm\Omega^2/\hbar^2 R_0\Delta^2)\right]$, and the BO approximation is valid for $\Delta^2/\Omega^2 < Dm/\hbar^2 R_0$. This condition competes with the weak coupling constraint $\Omega^2/\Delta^2 < 1$. However, for $\Omega/\Delta \sim 0.1$, both conditions can be satisfied for strong dipole interactions with $r_d > 100$.

The use of additional microwave fields coupling to the $|1, \pm 1\rangle$-states with detuning $\Delta_\perp \gg \Delta$ and Rabi frequency $\Omega_\perp$ allows for further shaping the effective potentials. One such example is shown in Fig.1(a), where $V_{\rm eff}^{\rm 2D}$ in the long range part $R > R_0$ becomes attractive and allows for the existence of bi-molecular bound states.

Finally, we can extend the above discussion to a gas of cold polar molecules confined into 2D with temperature $T < \hbar\omega_\perp$, and obtain the *many body Hamiltonian* [12]

$$H = \sum_i \frac{\mathbf{p}_i^2}{2m} + \sum_{i<j} V_{\rm eff}^{\rm 2D}(\mathbf{R}_i - \mathbf{R}_j). \quad (4)$$

The first term accounts for the kinetic energy within the x,y-plane, while the second term denotes the effective interaction potential with the strong repulsion $\sim D/R^3$ on short distances $r < R_0$, see above. The validity of this effective Hamiltonian requires that tunneling events through the barrier of the interparticle potential are suppressed, i.e., strong interactions and tight confinement with $Dm/\hbar^2 a_\perp \gg 1$. In turn, for decreasing interactions, tunneling through the barrier takes place and three body recombinations become relevant driving a crossover into a potentially unstable regime (note, that the approach towards this intermediate region from the weakly interacting side has been previously discussed [5]). The Hamiltonian Eq. (4) gives rise to novel quantum phenomena, which have not been accessed so far in the context of cold atoms/molecules. As an illustration, we focus on the interaction $V_{\rm eff}^{\rm 2D}(\mathbf{R}) = D/R^3$ with the dimensionless parameter $r_d = Dm/\hbar^2 a$ and the particle density $n = 1/a^2$. In the following, we present a tentative phase diagram of the system, see Fig. 3, and show that for realistic experimental parameters the polar molecules can be driven from the superfluid into the crystalline phase.

In the limit of strong interactions $r_d = Dm/\hbar^2 a \gg 1$ the polar molecules are in a crystalline phase for temperatures $T < T_m$ with $T_m \approx 0.09D/a^3$ [8]. The configuration with minimal energy is a triangular lattice with spacing $a_{\rm L} = (4/3)^{1/4}a$. The excitations are two linear sound modes with characteristic phonon frequency $\omega_p = \sqrt{D/a^5 m}$. The static structure factor S diverges at a reciprocal lattice vector $\mathbf{K}$, and $S(\mathbf{K})/N$ acts as an order parameter for the crystalline phase. In the opposite limit of weak interactions $r_d < 1$, the ground state is a superfluid (SF) with a finite (quasi) condensate. The SF is characterized by a superfluid fraction $\rho_s(T)$, which depends on temperature T, with $\rho_s(T = 0) = 1$. For finite temperature, a Berezinskii–Kosterlitz–Thouless transition towards a normal fluid is expected to occur at $T_{\rm KT} = \pi\rho_s\hbar^2 n/2m$. In turn, very little is known on the intermediate strongly interacting regime with $r_d \gtrsim 1$; see [9] for a discussion in 1D. Here, we focus on this intermediate regime and determine the critical interaction strength $r_{\rm QM}$ for the quantum melting transition. We use a recently developed PIMC-code based on the Worm algorithm [10]. In Fig. 3(d-e), the order parameters ρ_s and $S(\mathbf{K})/N$ are shown at a small temperature $T = 0.014D/a^3$ for different interaction strengths r_d and particle numbers $N = 36, 90$. We find that ρ_s exhibits a sudden drop to zero for $r_d \approx 15$, while at the same position $S(\mathbf{K})$ strongly increases. In addition, we observe that in a few occasions ρ_s suddenly jumped from 0 to 1, and then returned to 0, in the interval $r_d \approx 15 - 20$,
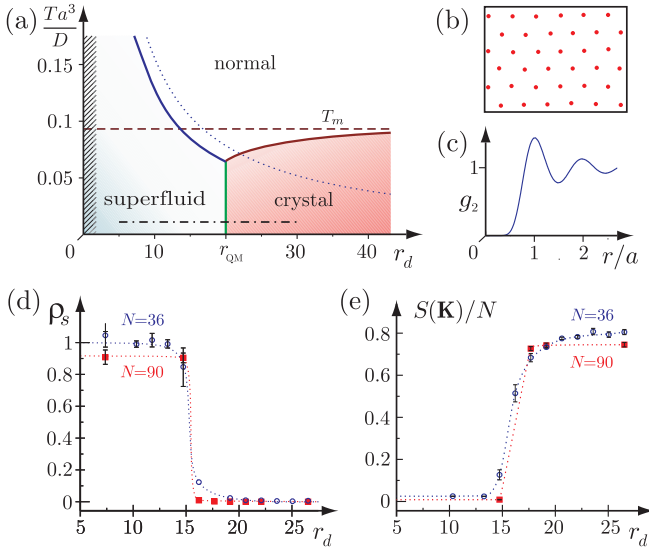
FIG. 3: (a) Tentative phase diagram in the $T - r_d$ plane: crystalline phase for interactions $r_d > r_{QM}$ and temperatures below the classical melting temperature T_m (dashed line). The superfluid phase appears below the upper bound $T < \pi\hbar^2 n/2m$ (dotted line). The quantum melting transition is studied at fixed temperature $T = 0.014D/a^3$ with interactions $r_d = 5 - 30$ (dash-dotted line). The crossover to the unstable regime for small replusion and finite confinement $\omega_\perp$ is indicated (hatched region). (b) PIMC-snapshot of the mean particle positions in the crystalline phase for $N = 36$ at $r_d \approx 26.5$. (c) Density-density (angle-averaged) correlation function $g_2(r)$, for $N = 36$ at $r_d \sim 11.8$. (d) Superfluid density ρ_s and (e) static structure factor $S(\mathbf{K})/N$ as a function of r_d, for $N = 36$ (circles) and $N = 90$ (squares).

which suggests a competition between the superfluid and crystalline phases. These results indicate a superfluid to crystal phase transition at $r_{QM} = 18 \pm 4$. The step-like behavior of ρ_s and $S(\mathbf{K})/N$ is consistent with a first order phase transition. For $r_d > r_{QM}$ the crystalline structure is triangular, in agreement with the discussion above, see Fig. 3(b). Note, that the superfluid with $r_d \sim 1$ is strongly interacting, in particular, the density-density correlation function is quenched on lengths $R < a$, see Fig. 3(c). Moreover, the (quasi) condensate involves a fraction of the total density, and therefore small coherence peaks in a time of flight experiment are expected. However, the detection of vortices can be used as a definitive signature of superfluidity, while Bragg scattering with optical light allows for probing the crystalline phase.

While many of the molecular species studied at present in the lab are candidates for observing the above phenomena, we note that e.g. SrO has a large dipole moment $d = 8.9D$ and allows optical trapping with a red detuned laser with wave length $\lambda \sim 1\mu m$. Then, for a trapping potential with $a_\perp \sim 50$nm and interparticle distance $a \sim 300$nm, we obtain $r_d \sim 410 \gg r_{QM}$, and the tunneling rate is suppressed with $d^2m/\hbar^2a_\perp \sim 2500$. Since the

classical melting occurs at $T_m(r_d = 400) \sim 2\mu K$, this molecule is a candidate to reach the quantum regime.

In conclusion, we have shown that cold polar molecules allow to extend the control of interactions in cold gases to the *shape* of the inter-particle potential, which opens a route towards generation of (novel) strongly correlated quantum phases in low dimensional trapping geometries. In particular, we have discussed the appearance and properties of a crystalline phase, and an associated quantum phase transition to a dipolar quantum gas. Besides the fundamental interest of observing crystal phases with neutral particles in atomic and molecular physics, the properties of dipolar molecular crystals might lead to interesting applications: these crystals appear in the high density limit, i.e. for small interparticle separation, which could potentially be smaller than optical lattice structures. At the same time, crystal phases are expected to be stable in the sense that (possibly damaging) short range collisions are suppressed.

[1] Nature insight: ultracold matter, Nature **416**, 205 (2002)
[2] See e.g. Special Issue on ultracold polar molecules, Eur. Phys. J. D **31**, 149-445 (2004); J. M. Sage, *et al.*, Phys. Rev. Lett. **94**, 203001 (2005); T. Rieger, *et al.*, *ibid.* **95**, 173002 (2005); D. Wang, *et al.*, *ibid.* **93**, 243005 (2004); S. Y. T. van de Meerakker, *et al.*, *ibid.* **94**, 023004 (2005); S. D. Kraft, *et al.*, arXiv:physics/0605019.
[3] C. Ticknor and J. L. Bohn, Phys. Rev. A **72**, 032717 (2005); R. V. Krems, Phys. Rev. Lett. **96**, 123202 (2006).
[4] K. Goral, L. Santos, and M. Lewenstein, Phys. Rev. Lett. 88, 170406 (2002); M. A. Baranov, K. Osterloh, and M. Lewenstein, *ibid.* **94**, 070404 (2005); E. H. Rezayi, N. Read, and N. R. Cooper, *ibid.* **95**, 160404 (2005); A. Micheli, G. K. Brennen, and P. Zoller, Nature Physics **2**, 341 (2006).
[5] K. Goral, K. Rzazewski, and T. Pfau, Phys. Rev. A **61**, 051601(R) (2000); L. Santos, G. V. Shlyapnikov, and M. Lewenstein, Phys. Rev. Lett. **90**, 250403 (2003); J. Stuhler, *et al.*, *ibid.* **95**, 150406 (2005).
[6] B. Friedrich and D. Herschbach, Phys. Rev. Lett. **74**, 4623 (1995); S. Kotochigova and E. Tiesinga, Phys. Rev. A **73**, 041405(R) (2006).
[7] J. Weiner, *et al.*, Rev. Mod. Phys. **71**, 1 (1999).
[8] R. K. Kalia and P. Vashishta, J. Phys. C **14**, 643 (1981).
[9] A. S. Arkhipov, *et al.*, JETP Lett. **82**, 39 (2005).
[10] M. Boninsegni, N. Prokof'ev, and B. Svistunov, Phys. Rev. Lett. **96**, 070601 (2006).
[11] For a sinusoidal $\mathbf{E}(t)$ a diagonalization precludes a transformation to a time-independent Floquet Hamiltonian.
[12] Three body interactions can be important for particles approaching each other on distances $|\mathbf{R}_i - \mathbf{R}_j| \sim R_0$, but these corrections are dropped in the following.